

Supporting Information

Self-Epitaxial Hetero-Nanolayers and Surface Atom Reconstruction in Electrocatalytic Nickel Phosphides

Xian-Kui Wei,^{*,†} Dehua Xiong,^{‡,§} Lifeng Liu,[‡] and Rafal E. Dunin-Borkowski[†]

[†]Ernst Ruska-Centre for Microscopy and Spectroscopy with Electrons, Forschungszentrum Jülich GmbH, Jülich 52428, Germany

[‡]International Iberian Nanotechnology Laboratory (INL), Braga 4715-330, Portugal

[§]State Key Laboratory of Silicate Materials for Architectures, Wuhan University of Technology, Wuhan 430070, China

*Correspondence author E-mail: x.wei@fz-juelich.de (X.K.W.)

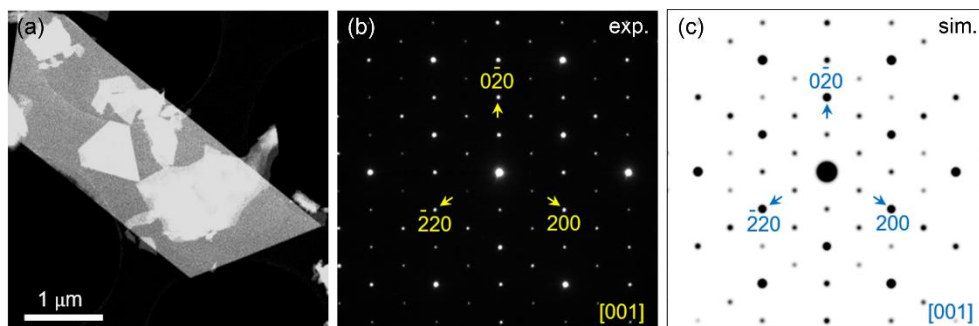


Figure S1. (a) Representative HAADF-STEM image of Ni_5P_4 nanosheets with preferential [001] orientation (one or two out of 20). (b,c) Selected area electron diffraction of Ni_5P_4 recorded along the [001] direction and the simulated one, respectively. Apart from the $\langle 2\bar{4}0 \rangle^*$ diffraction spots, the $\langle 100 \rangle^*$ diffraction spots show dramatic difference in intensity distribution in the reciprocal space. Being consistent with the high-resolution TEM and STEM results, the difference from the simulated electron-diffraction pattern also indicate clear features of surface atom reconstruction on the Ni_5P_4 nanosheets.

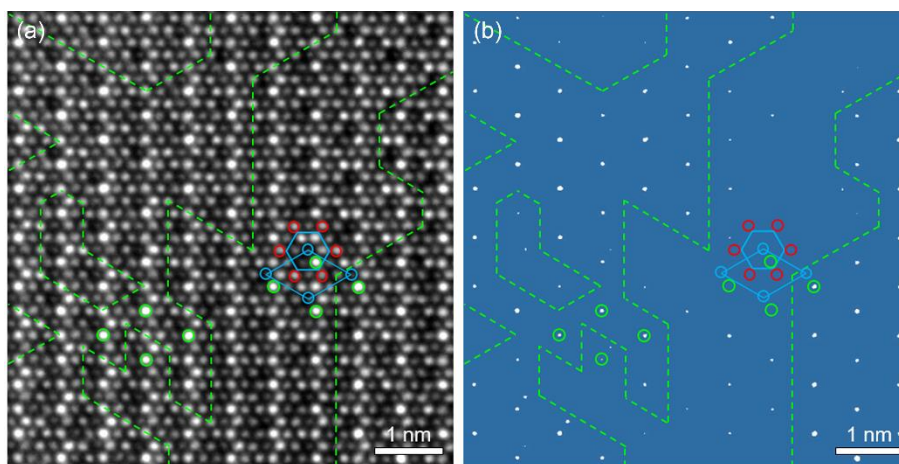


Figure S2. (a) A large-area view of the atomic-resolution TEM image presented in Figure 2c. It should be noted that the image intensity is normalized by a reference image recorded from a vacuum region under the same conditions during the experiments. (b) A filtered image of (a) via a certain intensity range ($I_{\max} - 1.05 \sim I_{\max}$) with respect to the maximum image intensity ($I_{\max} = 3.46$). From the $5\pi/3$ -point columns (green circles), we can clearly see different intensity distribution over this local image area. This clearly reveals presence of atomic steps on surfaces of the Ni₅P₄ nanosheets.

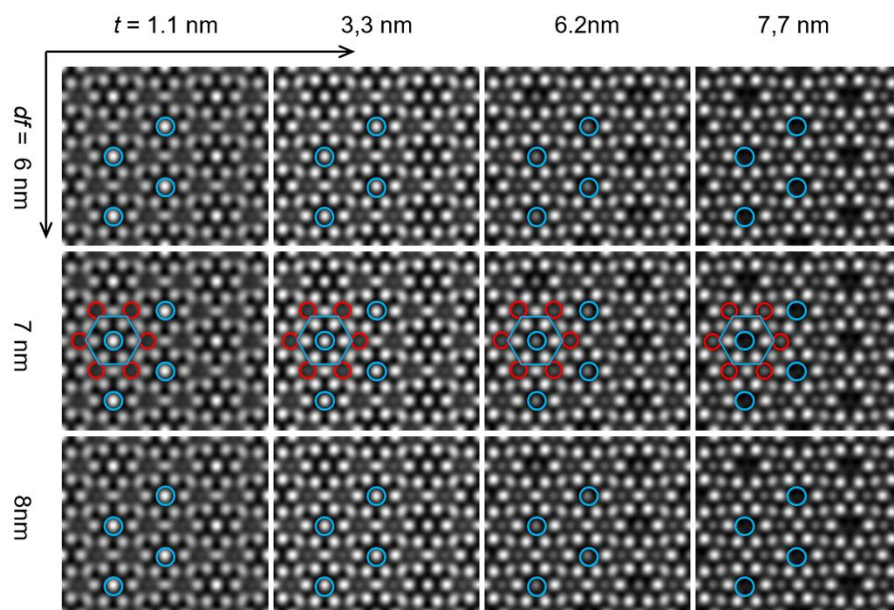


Figure S3. Simulated TEM image of Ni_5P_4 along the $[001]$ direction. Positions of the CNP and pure P atom columns are marked by green and red circles. With increasing of the specimen thickness, we can clearly see monotonic decreasing of intensity for the CNP columns. This feature is unchanged in the illustrated defocus range ($df = 6, 7$ and 8 nm). Apart from this, we see that the intensities of six-fold-symmetric NCNP columns keep equivalent under each of the thickness and defocus condition. With increasing of the specimen thickness, we also see monotonic increase of column intensity for the six-fold-symmetric pure P atoms along this direction.

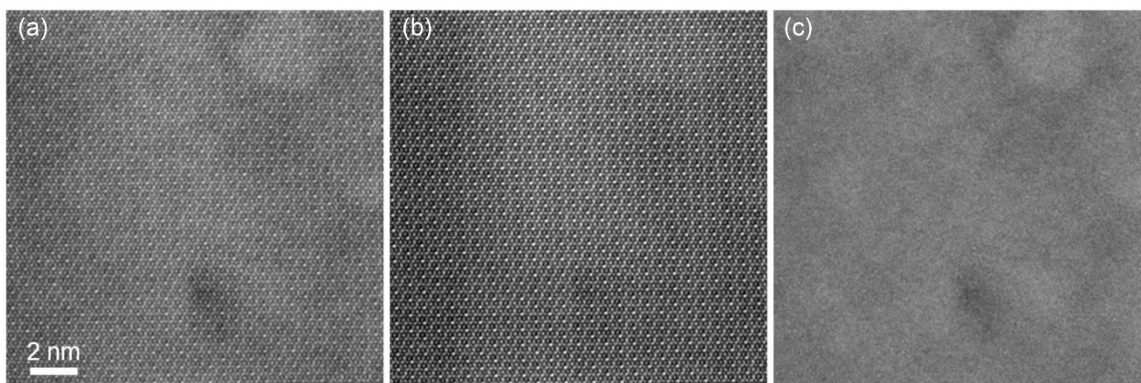


Figure S4. (a) Original atomic-resolution HAADF-STEM image of [001]-oriented Ni₅P₄ nanosheet. (b) Filtered HAADF-STEM image with removal of signal from the amorphous by a Wiener or average background subtraction. (c) Difference between the original and filtered image. From this image area, we clearly see a homogeneous distribution of reconstructed Ni atoms on the phosphide surface. After removal of the signal from the amorphous, several smaller regions of interest in (b) are selected and averaged to further improve signal-to-noise ratio. The averaged image is presented in Figure 2a.

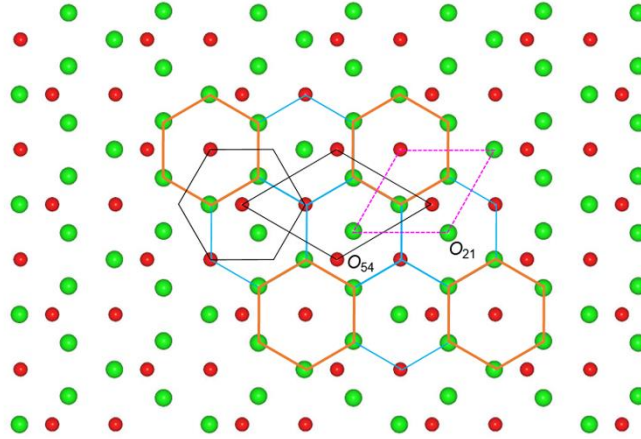


Figure S5. Structural model of Ni_3P_2 sublayer of Ni_5P_4 viewed along $[001]$ direction. The black parallelogram and largest hexagon denote the PUC and ETUC of Ni_5P_4 . The pink dashed parallelogram and smaller hexagons (orange and blue) denote the PUC and ETUC of Ni_2P . Repartition of the Ni_3P_2 sublayer by the ETUCs of Ni_2P also shows two kinds of $\text{ETUC}_{\text{S}21}$, the orange hexagons with a composition of Ni_2P_1 and the linking blue hexagons with a composition of $\text{Ni}_{7/3}\text{P}_{5/3}$. From the atomic occupation in this sublayer, one can see that none of the $\text{ETUC}_{\text{S}21}$ have similarity to any sublayer of Ni_2P . Compared with the Ni_3P_3 and Ni_4P_3 terminations, this suggests that the Ni_3P_2 is not a favorable termination for epitaxial growth of Ni_2P on top of Ni_5P_4 .

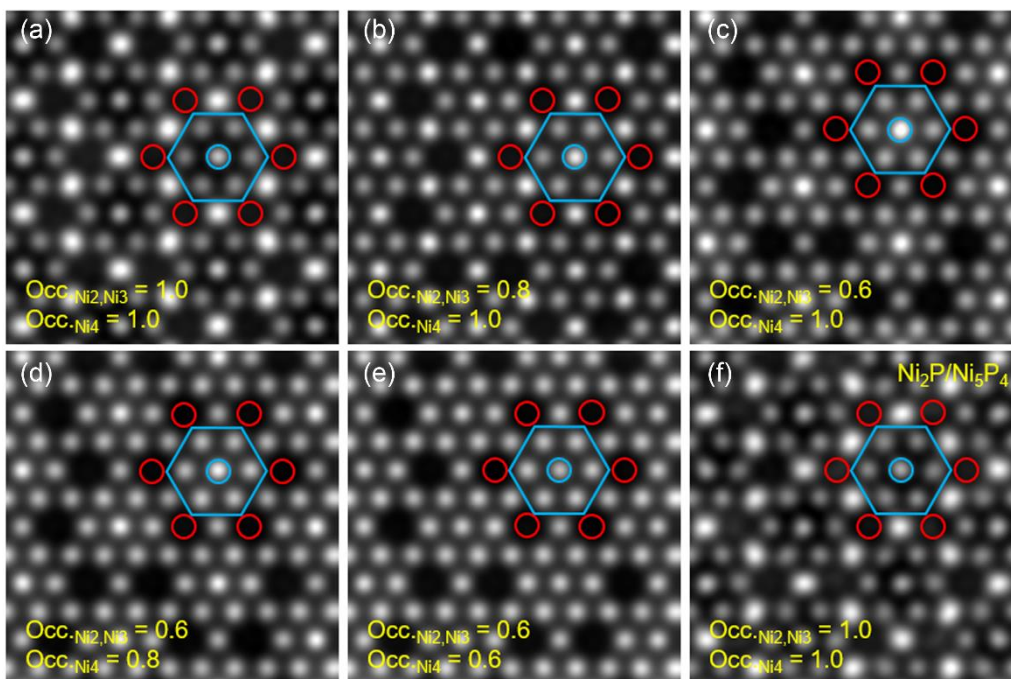


Figure S6. Simulated HAADF images of Ni_5P_4 with different Ni occupation and overlapping of Ni_2P on top along [001] direction. (a-c) Simulated HAADF images with occupation (Occ.) of Ni2- and Ni3-site atoms at 1.0 (a), 0.8 (b) and 0.6 (c) with $\text{Occ}_{\text{Ni4}} = 1.0$. (d,e) Image simulation with occupation (Occ.) of Ni2- and Ni3-site atoms setting as $\text{Occ.} = 0.6$ while $\text{Occ}_{\text{Ni4}} = 0.8$ and 0.6, respectively. (f) Simulated image of Ni_2P (2.2nm)/ Ni_4P_3 - Ni_5P_4 (38.5nm) along [001] direction with full occupation of all atoms.

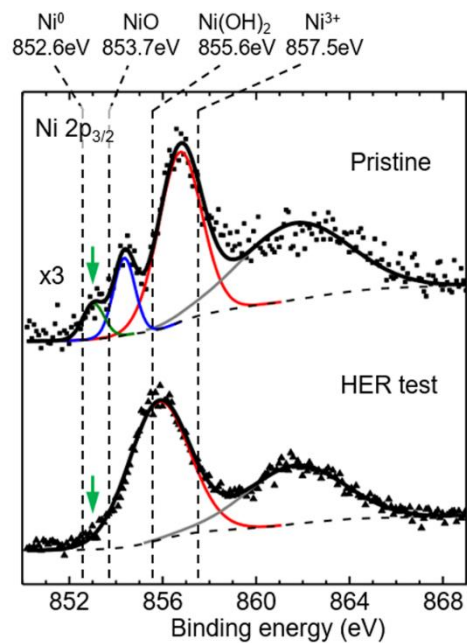


Figure S7. XPS spectra of Ni $2p_{3/2}$ for the Ni_xP_y nanosheets before and after the HER test.

The peaks are fitted based on simple models. For ease of comparison, typical binding energies about Ni-containing species are marked out. The Ni valence (green arrows) in the range of 0 ~1 suggests reconstruction of Ni atoms with P and other relevant atoms on the phosphide surfaces.

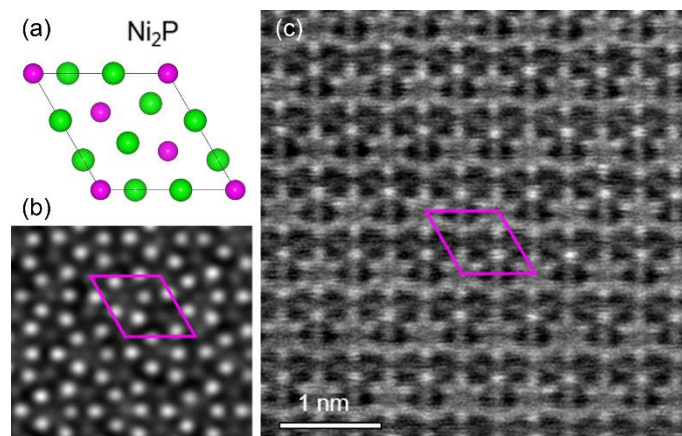


Figure S8. (a,b) Crystal structure and simulated HAADF-STEM image of Ni₂P along the [001] direction. (c) Atomic-resolution HAADF image of Ni₂P collected along the [001] direction. Corresponding to the enriched Ni detected by EDX, difference of the atom-column features between experimental and simulated images also evidences reconstruction of Ni atoms on surfaces of the Ni₂P phase. This further supports reconstruction of NiP_x ($0 < x < 0.5$) on top of Ni₂P-covered Ni₅P₄ phase.

Table S1. Atomic position, Debye-Waller factor and occupation of atoms in Ni₅P₄ and Ni₂P used for quantitative image simulation.

Phase	Atom	x	y	z	B/[Å ²]	Occ.
Ni ₅ P ₄ Lattice parameter <i>a</i> = 0.67894 nm <i>c</i> = 1.0989 nm	Ni1	0.1778	0.8222	0.2365	0.44	1.0
	Ni2	0.5057	0.4943	0.0872	0.44	0.6
	Ni3	0.5118	0.4882	0.3775	0.44	0.6
	Ni4	0.0000	0.0000	0.1989	0.42	0.8
	P1	0.1567	0.8433	0.4406	0.43	1.0
	P2	0.8391	0.1609	0.2306	0.47	1.0
	P3	0.3333	0.6667	0.0556	0.36	1.0
	P4	0.0000	0.0000	0.0000	0.39	1.0
Ni ₂ P Lattice parameter <i>a</i> = 0.5880 nm <i>c</i> = 0.3382 nm	Ni1	0.2575	0.0000	0.5000	0.45	1.0
	Ni2	0.5957	0.0000	0.0000	0.45	1.0
	P1	0.3333	0.6667	0.5000	0.50	1.0
	P2	0.0000	0.0000	0.0000	0.50	1.0